EUROPEAN ORGANIZATION FOR NUCLEAR RESEARCH

CERN-EP/82-73
10 June 1982

HADRONIZATION OF EXCITED NUCLEONS IN NUCLEAR COLLISIONS AT ISR ENERGIES

The Axial Field Spectrometer Collaboration

(BNL[1]-CERN[2]-Copenhagen[3]-Lund[4]-Pennsylvania[5]-RAL[6]-Tel Aviv[7])

T. Åkesson[4], M.G. Albrow[6], S. Almehed[4], O. Benary[7], H. Bøggild[3], O. Botner[2], H. Brody[5], V. Burkert[2], A. Di Ciaccio[1], D. Cockerill[6], S. Dagan[7], E. Dahl-Jensen[3], I. Dahl-Jensen[3], G. Damgaard[3], W.M. Evans[6], C.W. Fabjan[2], S. Frankel[5], W. Frati[5], H. Gordon[1], A. Hallgren[2], K.H. Hansen[3], B. Heck[2], H.J. Hilke[2], J.E. Hooper[3], G. Jarlskog[4], P. Jeffreys[6], G. Kesseler[2], T. Killian[1], J. v.d. Lans[2], P.R. Lindblom[5], D. Lissauer[7], B. Lörstad[4], T. Ludlam[1], L. Madansky[8], N.A. McCubbin[6], A. Melin[4], U. Mjornmark[4], R. Møller[3], W. Molzon[5], B.S. Nielsen[2], A. Nilsson[4], L.H. Olsen[2], Y. Oren[7], L. Rosselet[2], E. Rosso[2], A. Rudge[2], R.H. Schindler[2], B. Schistad[3], W.J. Willis[2], M. Winik[1], J.J. Winterberg[5], W. Witzeling[2], C. Woody[1].

(Submitted to Nuclear Physics B)

1. Brookhaven National Laboratory, USA *
2. CERN, Geneva, Switzerland
3. Niels Bohr Institute, University of Copenhagen, Denmark
4. University of Lund, Sweden
5. University of Pennsylvania, USA*
6. Rutherford Appleton Laboratory, UK
7. University of Tel-Aviv, Israel
8. Johns Hopkins University, USA *

* Supported in part by U.S. Department of Energy

ABSTRACT

Calorimeters downstream of the intersection of $p\alpha$ and $\alpha\alpha$ beams in the ISR have been used to study the hadronization of excited nucleons. These data extend and support the conclusions from previous studies of the A-dependence of particle multiplicities in ultrarelativistic p-nucleus collisions, which provided evidence that the proton hadronizes outside the nuclear volume.

1. INTRODUCTION

It is normally assumed that the hadronization time, i.e. the mean time which elapses between the excitation of a hadron and its hadronization into pions, kaons, etc., is greater than the ratio of the hadronic size to the velocity of light. In a p-nucleus collision, viewed from the nuclear frame, this time is dilated by the Lorentz factor, γ, which at ISR energies is about 1000. One can therefore expect that the hadronization of the incoming proton will take place well outside the nuclear volume. Of course, the hadronization of the struck nucleon in the nucleus will take place inside that nucleus if their relative velocities are small.

There is excellent indirect evidence [1] that this is indeed the case. This evidence comes from a study of the A-dependence of the multiplicity observed in p-nucleus collisions. The study of ref. 1 showed that in the fragmentation region of the incoming proton, i.e. at small forward angles, the multiplicity was independent of A. This supports the view that the proton hadronizes outside the nuclear volume, since otherwise the large number of pions produced would cascade in a strongly A-dependent way. Even though the incoming proton might interact strongly with several nucleons in the nucleus (and the mean free path is short enough so that it surely must), it appears to hadronize, to a good approximation, into the same multiplicity of hadrons as that observed in a pp interaction. One would like to verify this behaviour in other ways since it provides a constraint on any theory of hadron-hadron or hadron-nucleus interactions.

The proton projectile passing through the nucleus can undergo three effects not present in pp scattering. Firstly, there is the possibility of multiple scattering, resulting in an added spread of the secondaries about the collision axis. Secondly, there is the effect of the transverse component of the Fermi momentum in the nucleus. The multiplicity measurements alone would not be sensitive to these effects. Thirdly, there is the possibility that the projectile, interacting a second or third time, might hadronize into a different number of pions than in a single encounter. Apparently this is not observed, and if it does exist it must be a small effect. If the multiplicity increased or decreased as a result of multiple collisions, ref. 1 would have seen a departure from the A-independence of proton fragmentation.

The multiplicity measured in the fragmentation region of the nucleus is in complete agreement with this picture. Here we expect the multiplicity to increase with A, but only to increase as the effective path length which varies as $A^{1/3}$. This is precisely the A-dependence found in ref. 1. Apparently, even though these nucleons hadronize within nuclear matter, the soft rescatterings that are expected to occur do not appreciably affect the multiplicity since such effects would lead to a stronger A-dependence. Contributions from the hadronization of both the proton and the target nucleons should be observed at zero rapidity in the pN c.m. frame. Here the A-dependence is intermediate between that observed in the two fragmentation regions.

These multiplicity studies are in agreement with the expected dilation of the hadronization time and, in addition, show how studies with nuclei can give information that cannot be obtained directly from studies of the pp interaction. The results also suggest that in pp interactions at these high energies each excited proton hadronizes far from its initial interaction point.

The dilation of the hadronization time should also have unique effects on the nuclear physics aspects of nucleus-nucleus collisions. One of the difficulties in predicting nucleus-nucleus interactions from p-nucleus interactions at energies of only a few GeV/nucleon, as at Berkeley or Dubna energies, comes about because the dilation is negligible. Soft rescatterings of the nucleon and scattering or absorption of the hadronization products (mainly pions) in a pA collision occur in nuclear matter containing A+1 nucleons, while in AA collisions the rescatterings occur in nuclear matter containing 2A nucleons. Thus there is no clean way to compare the reactions when the poorly known final-state interactions are significant. However, at ISR energies the hadronization and subsequent rescatterings always take place in a system of A nucleons. Whether or not a nucleon in a nucleus A is struck by a proton or another nucleus A′ it hadronizes in the same environment, i.e. among A nucleons.

Because of the importance of this relativistic effect, it appears desirable to obtain additional experimental information to supplement that derived from the A-dependence of the multiplicities. In our recent experiments on pp, pα, and $\alpha\alpha$ collisions at the ISR we have been able to compare various properties of the hadronization of both protons and α-particles and, for the first time at such high energies, to compare the hadronization of nucleons in an α-particle traversing either a proton or another α-particle. These results are the subject of this paper. The method we have used is to measure the products of the inelastic interactions, using calorimeters sensitive to both charged and neutral particles in the fragmentation regions.

2. EXPERIMENTAL ARRANGEMENT

Figure 1 shows the pertinent parts of the apparatus, which was located at the I8 intersection at the ISR. Surrounding the vacuum pipe on each downstream side of the intersection region are calorimeters which detect most of the hadronization fragments that leave the vacuum pipe. The calorimeters [2] are made up of eight modules each 0.21 m × 0.51 m × 0.8 m. The front face of each calorimeter is located 4.5 m from the intersection. At 5.0 m the calorimeter subtends an angle of approximately 0.1 rad. The central modules are located 50 mm above and below the beam, which measured 6 mm (vertically) × 60 mm (horizontally) at the entrance to the calorimeter.

Each of the identical modules is constructed of alternate layers of scintillators and copper sheets normal to the entrance direction. Light in the scintillators passes in the +x/−x directions to wavelength shifter sheets on each side of the module, each viewed by a photomultiplier. The calorimeters have an energy resolution $\sigma_E/E = 0.01E^{\frac{1}{2}} + 0.45E^{-\frac{1}{2}}$ for hadrons. Measurement of the phototube pulse-height differences allows location of the centre-of-energy deposition in the x direction to an accuracy of a few centimetres. One can also bin the lateral energy deposition crudely by summing the pulse heights in the separate photomultipliers at the same x. This allows us to examine various features of the deposition of the hadronization products in the calorimeter. In front of the calorimeter is a four-quadrant hodoscope of scintillation counters, covering 19 mrad < θ < 90 mrad.

Figure 1 shows only one of the downstream arms, but the arrangement is symmetric about the intersection region. An event is recorded if at least one of the four sectors of the beam hodoscope in front of each of the calorimeters fires. This trigger is sensitive to about 60% of the inelastic cross-section in pp collisions at $\sqrt{s}$ = 63 GeV. Also shown is the "barrel" of 44 scintillation counters that can act as a hodoscope for triggering on central region multiplicity. Each of these counters covers 8° in azimuth, and their average rapidity coverage is ±1.7 units.

3. MEASUREMENTS

The plan of our study was to use the calorimeters to measure many features of the beam jets and to make comparisons between these features for protons interacting with either protons or α-particles. In this study we compare the fragmentation of 32 GeV protons "penetrating" 32 GeV protons with those penetrating 63 GeV α-particles. We then compare the fragmentation of nucleons travelling within an α-particle, for α-particles penetrating protons and α-particles penetrating α-particles.

The pulse heights from the phototubes are used to compute a series of quantities that characterize the deposition of energy in the calorimeters. These are (x is the horizontal coordinate, see fig. 1):

i) the pulse-height distribution summed over all eight modules,

ii) the average value of x summed over all the modules, x_{av}

$$x_{av} = \sum x_i E_i \Big/ \sum E_i \ ,$$

iii) the r.m.s. spread of x about x_{av},

$$x_{rms} = \sqrt{\sum (x_{av} - x_i)^2 \ E_i / \sum E_i} \ ,$$

iv) the average pulse height in the photomultipliers as a function of x (the upper and lower modules are summed),

v) the calorimeter module multiplicity distribution, requiring that the pulse height exceeds a minimum value in any module (0.5 GeV),

vi) the mean of the module multiplicity distribution for any total energy deposition in the total calorimeter.

Figure 2 shows a comparison of the pulse-height distributions in the p-side calorimeter for 32 GeV p - 32 GeV p and 32 GeV p - 63 GeV α collisions. The proton penetrating the α-particle deposits somewhat less energy in the calorimeter. The calorimeter pulse height is linear in energy to 2% [2], and from this figure we note that the most likely pulse height resulting from an inelastic 32 GeV p - - 32 GeV p collision is about 220 units. (For a 32 GeV proton entering the calorimeter directly it is 375 units.) Because of the presence of the beam pipe only inelastic protons with transverse momenta $\gtrsim$ 0.2 GeV/c enter the calorimeter.

Figure 3 shows the two calorimeter module multiplicity distributions (curves labelled "p-side") selecting a pulse height of 100 units on the proton side. The pp and pα distributions have essentially the same shape but with the pα case shifted to slightly lower multiplicities. The module multiplicity is determined by both energy deposition and particle multiplicity and should not be confused with particle multiplicity.

Figure 4 shows the mean module multiplicity versus pulse height, showing a small (7%) residual difference in the comparison at large pulse heights.

Figure 5 displays the lateral deposition of energy as evidenced by the pulse height in the photomultipliers versus x, the photomultiplier position. As in fig. 2 we see smaller pulse heights with slightly more lateral spreading in the pα case. The additional lateral spread in the pα case can come from two effects: Fermi motion in the α-particle and multiple proton scattering. This spreading may then account for the slightly lower pulse height in fig. 2, since more energy may miss the calorimeter.

One way to study this is to examine very low central multiplicity events so that one is reasonably sure that the proton only underwent a single inelastic scatter in the α-particle. The selection is carried out by use of the barrel counters, utilizing the number of scintillator hits to measure central multiplicity, i.e. for $|y| < 1.7$. The distributions for the two cases are shown in fig. 6.

There might be a slight indication of spread introduced by the initial internal momenta (Fermi motion) within the α-particle, but it appears to be smaller than the effect of multiple scattering observed in fig. 5.

Figure 7 shows accentuation of the multiple-scattering effect when the selection is made on high central multiplicity, $m > 10$. The ratio of the average pulse height in the outer modules to that in the central module is 0.90 in the pp case compared with 1.20 in the pα case (the systematic errors on these ratios being $\leq 5\%$). Figure 8 compares the distribution of the centre of energy x_{av}, for each event about the beam axis for pp and pα on the p-side. Figure 9 shows the distribution of r.m.s. spreads, x_{rms}, computed about the value of x_{av} for each event. Neither the x_{av} distribution nor the spread of energy about the x_{av} are very different in these pp and pα comparisons.

From these measurements we conclude that the energy distribution and spatial distribution of hadronization products of protons in pp and pα interactions, as measured with calorimeters in the fragmentation region, are very similar. The small differences observed may be attributed to Fermi motion in the α-particle and multiple-proton scattering. There is no sign of strong interaction of the hadronization products with the other nucleons in the α-particle.

4. ROLE OF "SPECTATORS" IN ALPHA COLLISIONS

Before we turn to a comparison of α-particles traversing protons or α-particles -- our final study -- we digress to discuss the role of "spectators".

In a collision in which, for example, a single nucleon in an α-particle has interacted, the other three nucleons, free, or bound as deuterons, tritons, or ^{3}He, do not have vanishing probability of remaining inside the beam pipe. The p_T distributions of deuteron, triton, and ^{3}He fragments are known from measurements with 1-2 GeV/nucleon heavy ions [3]. They show a Gaussian fall-off with transverse momentum with $\sigma = 0.14$ GeV/c. If those observed fall-offs had persisted to higher energies, the spectators would have been confined to the vacuum pipe in our arrangement. However, at ISR energies the multiplicities are larger and the larger number of pions, kaons, etc., tends to "blow apart" the residual fragments. There is evidence for this energy dependence from the comparison of 0.8 GeV and 400 GeV [4] inclusive cross-sections in the target fragmentation region. We have computed, in our geometry, and from the measured p_T distributions [5] that less than 0.4% of the inelastic events would have tritons or ^{3}He ions leaving the beam pipe and entering our calorimeters, but approximately 4% of the events can be contamination from deuterons. There are no data at present from which the contamination of "spectator" nucleons can be reliably calculated, but this contamination should be larger for two reasons: there are more single nucleons than deuterons in the final state and their longitudinal momenta are half as large.

Figure 10 shows a plot of the pulse-height distribution in the α-side calorimeters for both pα and αα inelastic collisions. For comparison the pulse-height distribution for 15 GeV inelastic pp collisions is shown. If the spectators were completely confined to the vacuum pipe the pα spectrum would have indicated the presence of an extremely high number of pN collisions in pα interactions, in contradiction with previous observations [1]. The large excess is due to the spectator contribution and hence it is this contribution which also accounts for the excess in the αα data.

The data do show more energy deposition in the αα case than in the pα case, as a result of the larger number of independent collisions. The presence of spectators precluded the possibility of determining the number of inelastic scatters from the calorimeter pulse heights in a simple way. This is unfortunate, since otherwise a measure of the energy deposition in forward calorimeters would have provided a model-independent estimate of the number of inelastic pN interactions. By contrast the determination of this number from central multiplicity distributions is highly model-dependent.

5. PRESENTATION OF THE αα DATA

We now turn to a study of α-particles traversing either a proton or another α-particle in an attempt to determine whether, in nucleus-nucleus interactions, the two nuclei hadronize outside the primary interaction region.

If the number of multiple hard collisions in both pα and αα collisions were the same or represented a small fraction of the events we could treat the "spectators" as a common background in studies of the pulse-height and energy distribution in the α-side calorimeter, since in both cases the final-state rescatterings that cause their ejection take place in an A = 4 environment. We shall assume that this is a reasonable approximation in the studies that follow, i.e. we assume that the contribution of spectators caused by the "blowout" is approximately the same in both cases.

Figure 3 (curves labelled "α-side") shows a comparison of the multiplicity distributions for a fixed calorimeter pulse height of 550, i.e. for an energy deposition of about 44 GeV. There is little difference in the two cases. Figure 11 shows the mean module multiplicity versus pulse height, figure 12 compares the lateral energy distribution, fig. 13 shows the x_{av} distribution, and fig. 14 shows the x_{rms} distribution. In all cases the α-particle fragmentation appears the same for αp and αα collisions.

Finally, we return to a comment on the experimental observation that the lateral spreads are quite different in the p-side (fig. 5) and α-side (fig. 12) comparisons. In the latter case the hadronization takes place within the α-particle. Since we know that the lateral spread due to the (final state) "blowing apart" of the α-particle far exceeds the Fermi motion spreading in the initial state, we should expect that the lateral spreads would be more similar in the αp and αα (α-side) comparisons. This effect is absent on the p-side. Now the Fermi motion in the pα case, absent in pp, shows up in the lateral spread. (Unfortunately, one cannot look for further confirmation in the direct comparison of the calorimeters on both sides in pα since the nucleons have different energies.)

6. CONCLUSIONS

We have used beam calorimeters, sensitive to hadronization into both charged and uncharged particles, to attempt to identify differences in the hadronization of protons or α-particles passing through proton or α-particle targets. The hadronization of protons in pα collisions appears to be very similar to that in pp collisions. In an attempt to compare the hadronization for the same number of nucleon scatters, $\alpha\alpha$ collisions are compared with αp collisions at the same energy. We find that all features of the calorimeter measurements in the α-particle fragmentation region are identical. The latter represent the first such studies of nucleus-nucleus interactions at extreme relativistic energies.

We believe these new calorimeter measurements support the accepted view, derived from measurements of the A-dependence of the multiplicities in the fragmentation region, that the relativistic dilation of the final-state evolution time ensures that the interacting particles hadronize far from the interaction region.

Acknowledgements

We acknowledge with thanks the work of the CERN Experimental Facilities Division on the calorimeter construction, and that of the ISR Experimental Support Group on the installation. We thank the PS and ISR Divisions for providing beams of α-particles in the ISR. Support from the Research Councils in our home countries is gratefully acknowledged.

REFERENCES

[1] W. Busza et al., Phys. Rev. Lett. 34 (1975) 836.

[2] O. Botner et al., Nucl. Instrum. Methods 179 (1981) 45.

[3] D.E. Greiner et al., Phys. Rev. Lett. 35 (1975) 152.

[4] S. Frankel et al., Phys. Rev. C 20 (1979) 2257.
N.A. Nikiforov et al., Phys. Rev. C 22 (1980) 700.

[5] M. Faessler, private communication on experiment R418. Forward deuterons and tritons were fit with Gaussian p_T distributions with $\sigma = 0.25 \pm 0.01$ GeV/c and 0.31 ± 0.02 GeV/c, respectively (preliminary).

Figure captions

Fig. 1 : View of the apparatus. Calorimeters are located 4.5 m from the intersection, surrounding both downstream beams (one shown) in the ISR I8 intersection. Four-quadrant scintillation hodoscopes precede each calorimeter, and a 44-element scintillation "barrel" hodoscope surrounds the intersection region.

Fig. 2 : Pulse-height distributions on the p-side in 31.5 GeV p - 31.5 GeV p and 31.5 GeV p - 63 GeV α collisions.

Fig. 3 : Relative number of events versus calorimeter module multiplicity. Left curves: multiplicity distributions in p-side calorimeter for a pulse height of 100; pp and pα comparison. Right curves: multiplicity distributions in α-side calorimeter for a pulse height of 550; $\alpha\alpha$ and pα comparison.

Fig. 4 : Mean calorimeter module multiplicity versus pulse height. The most probable pulse height for an elastically scattered 31.5 GeV proton is 375 units.

Fig. 5 : Lateral energy deposition. The photomultiplier pulse heights, averaged for upper and lower modules, versus the photomultiplier position. Vertical lines mark the edges of the calorimeter modules.

Fig. 6 : Lateral energy deposition for events with low central "barrel" multiplicities, M = 1,2.

Fig. 7 : Lateral energy deposition for events with high central "barrel" multiplicities, M > 10.

Fig. 8 : Distribution of the centre of energy, $x_{av} = \sum x_i E_i / \sum E_i$. The half width is ±15 cm.

Fig. 9 : Spread of energy in an event about the mean position

$$x_{rms} = \sqrt{\left(\sum (x_{av} - x_j)^2 E_i / \sum E_i\right)} .$$

Fig. 10 : Pulse height spectra on the α-side. The largest pulse heights correspond with 126 GeV energy deposition. The spectrum for inelastic 15 GeV pp collisions is shown as a smooth curve.

Fig. 11 : Mean calorimeter module multiplicity versus pulse height on the α-side. Solid lines sketch mean calorimeter multiplicities for 15 and 31 GeV pp collisions.

Fig. 12 : Lateral energy deposition (as in fig. 5) on the α-side.

Fig. 13 : Centre-of-energy distribution (as in fig. 8) on the α-side.

Fig. 14 : Energy spread about the centre of energy (as in fig. 9) on the α-side.

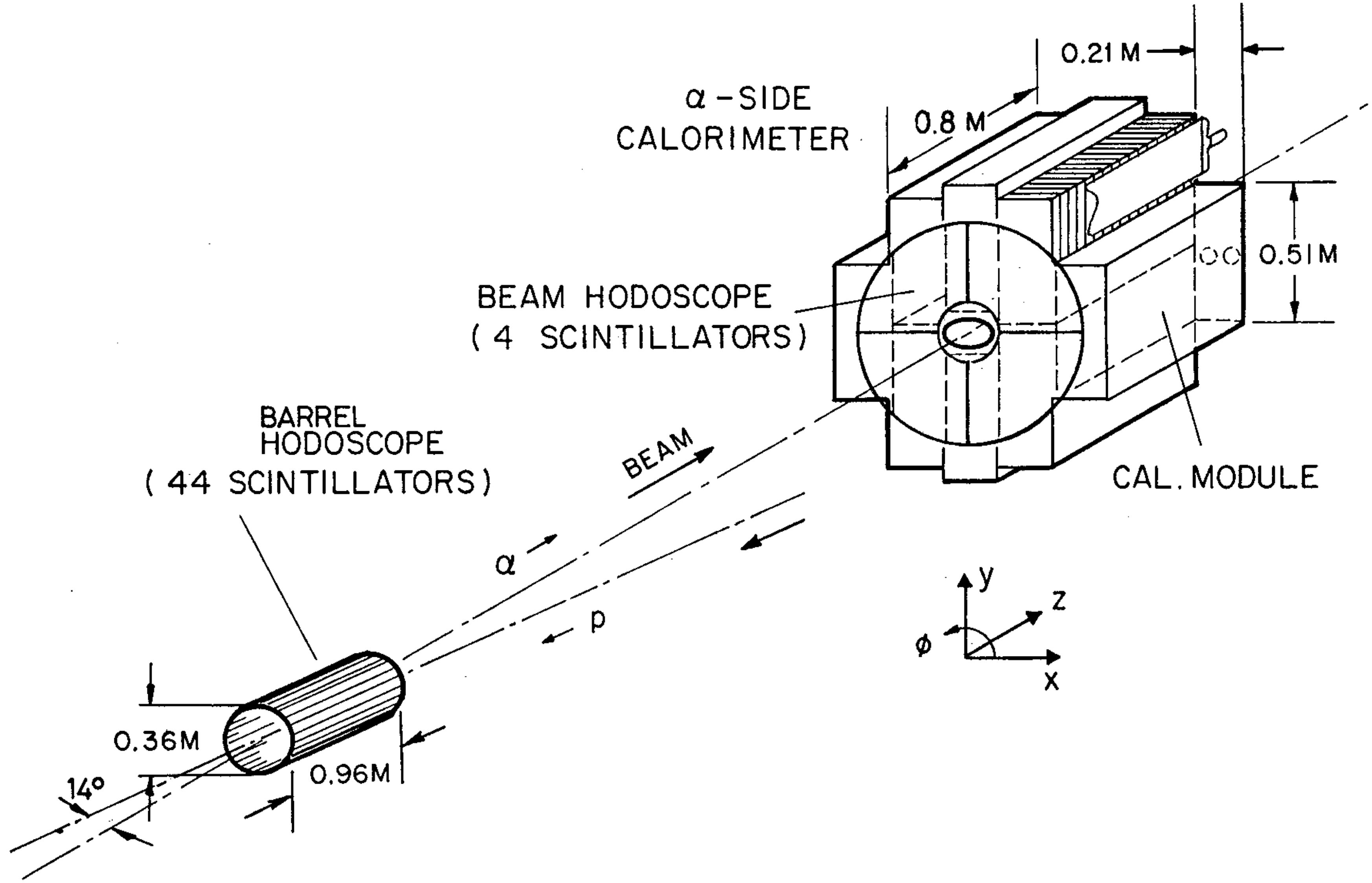
α -SIDE
CALORIMETER
0.8 M
0.21 M
0.51 M
BEAM HODOSCOPE
(4 SCINTILLATORS)
CAL. MODULE
BARREL
HODOSCOPE
(44 SCINTILLATORS)
BEAM
α
p
y
z
x
ϕ
0.36M
0.96M
14°

Fig. 1

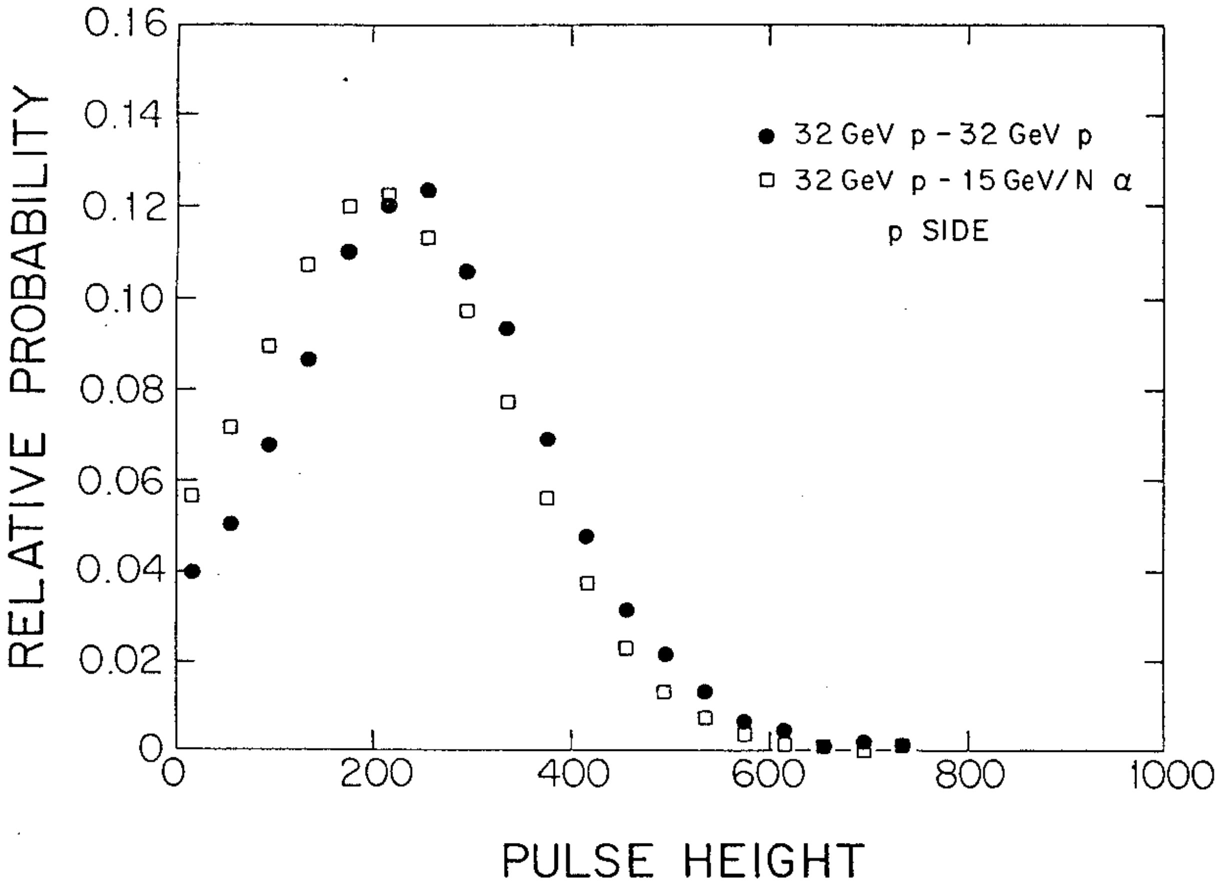
RELATIVE PROBABILITY
PULSE HEIGHT
32 GeV p - 32 GeV p
32 GeV p - 15 GeV/N α
p SIDE
0.16
0.14
0.12
0.10
0.08
0.06
0.04
0.02
0
0
200
400
600
800
1000

Fig. 2

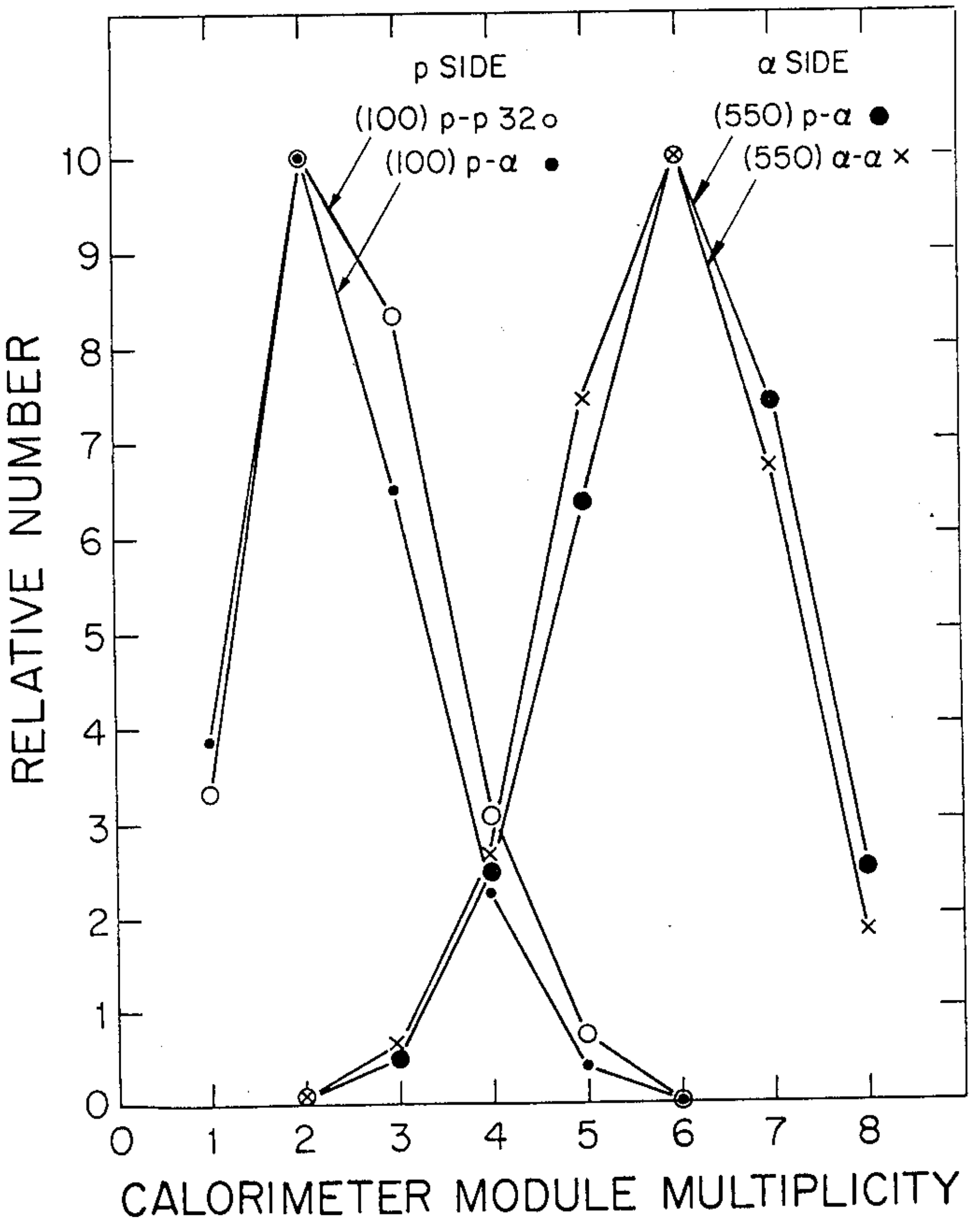
p SIDE
(100) p-p 32 o
(100) p-α •
α SIDE
(550) p-α ●
(550) α-α ×
RELATIVE NUMBER
0
1
2
3
4
5
6
7
8
9
10
CALORIMETER MODULE MULTIPLICITY

Fig. 3

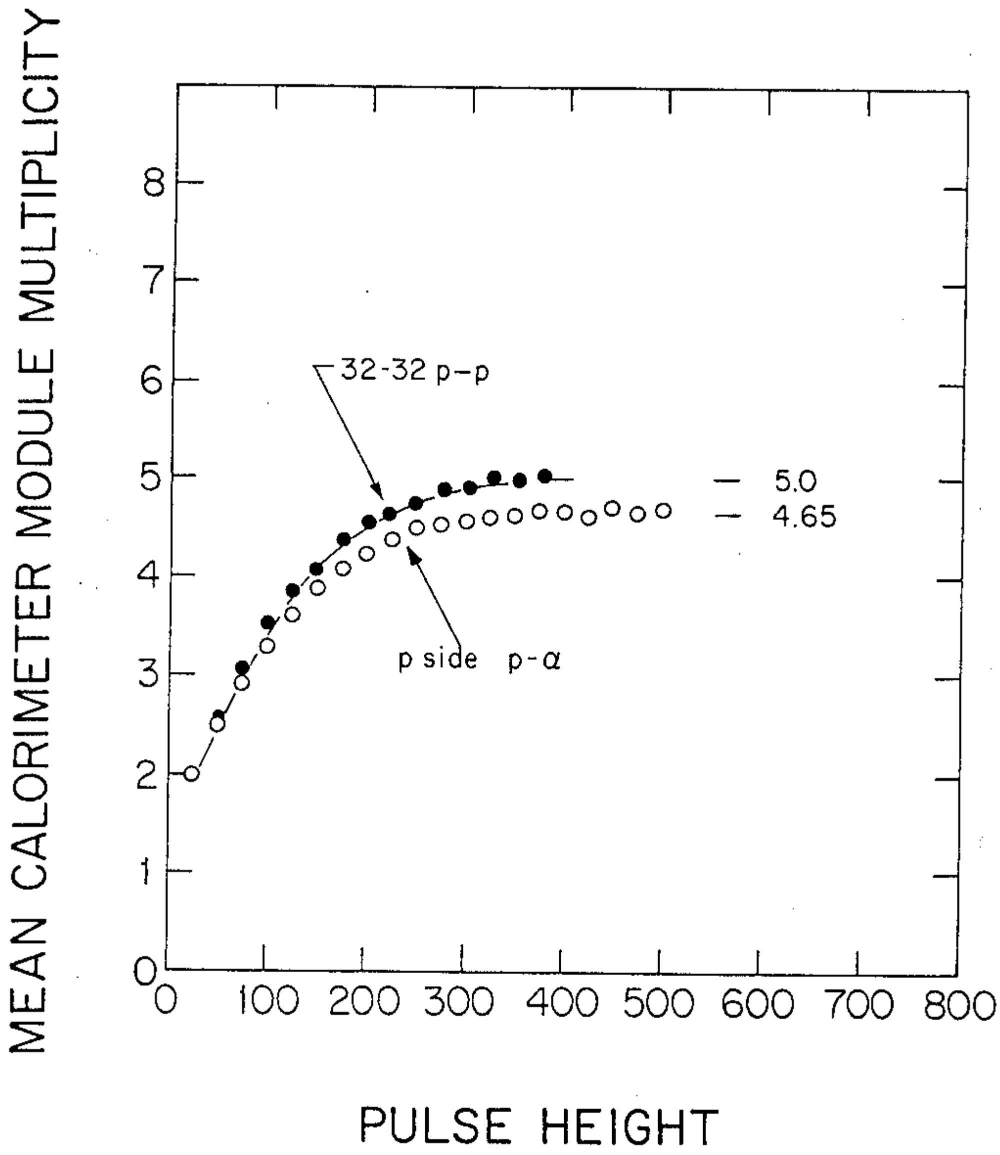
MEAN CALORIMETER MODULE MULTIPLICITY
0
1
2
3
4
5
6
7
8
0
100
200
300
400
500
600
700
800
PULSE HEIGHT
32-32 p-p
p side p-α
5.0
4.65

Fig. 4

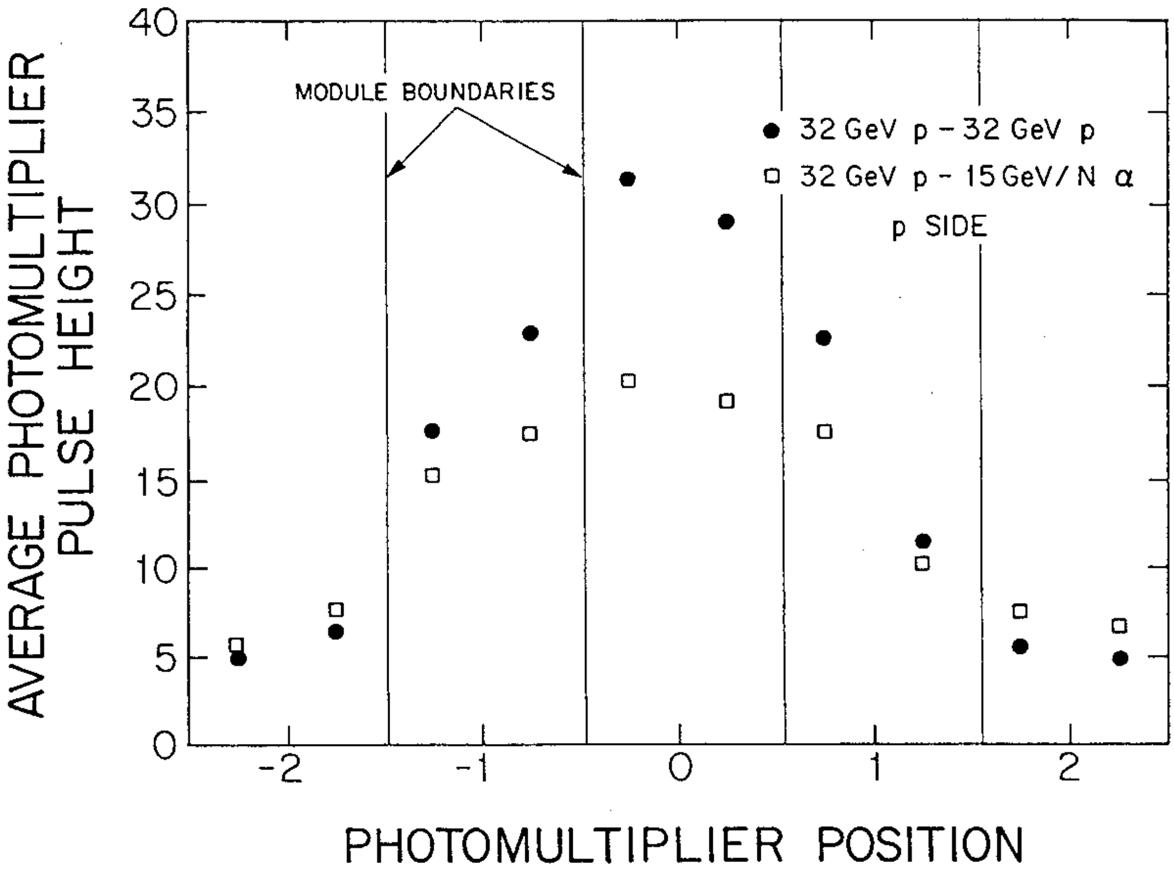

AVERAGE PHOTOMULTIPLIER PULSE HEIGHT
40
35
30
25
20
15
10
5
0
MODULE BOUNDARIES
32 GeV p - 32 GeV p
32 GeV p - 15 GeV/N α
p SIDE
-2
-1
0
1
2
PHOTOMULTIPLIER POSITION

Fig. 5

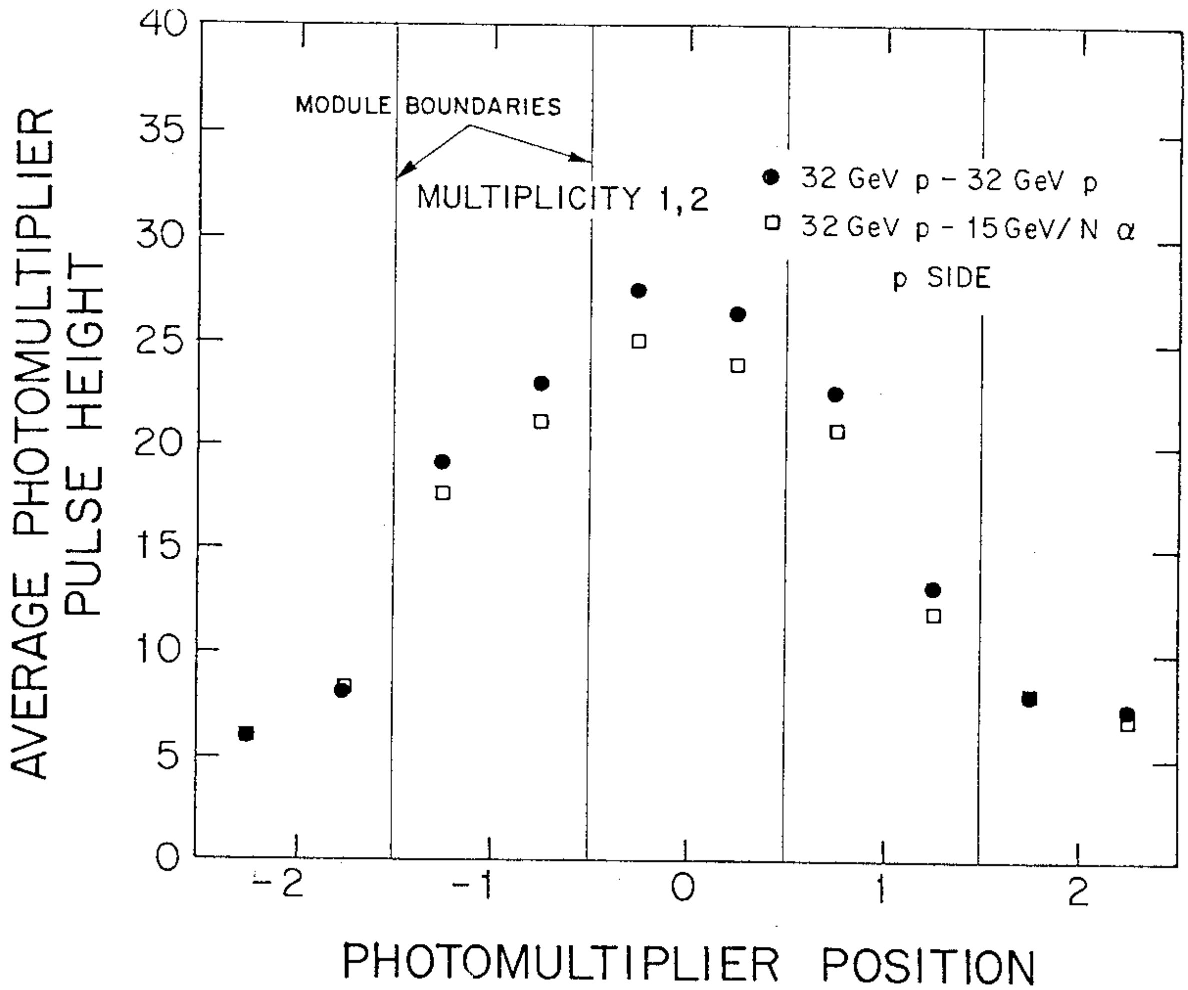

MODULE BOUNDARIES
MULTIPLICITY 1,2
● 32 GeV p - 32 GeV p
□ 32 GeV p - 15 GeV/N α
p SIDE
AVERAGE PHOTOMULTIPLIER PULSE HEIGHT
PHOTOMULTIPLIER POSITION

Fig. 6

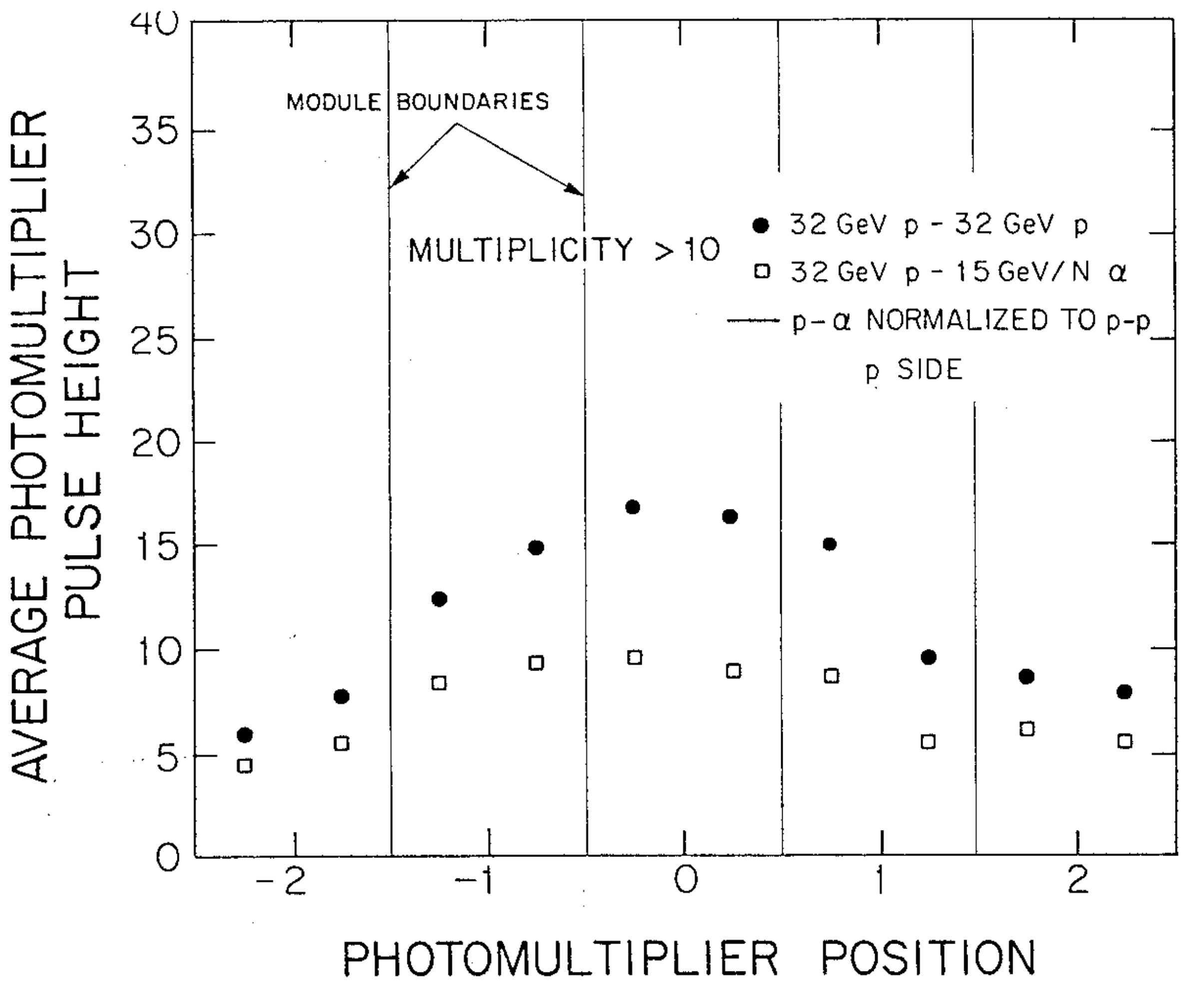
AVERAGE PHOTOMULTIPLIER PULSE HEIGHT
PHOTOMULTIPLIER POSITION
MODULE BOUNDARIES
MULTIPLICITY > 10
32 GeV p - 32 GeV p
32 GeV p - 15 GeV/N α
p-α NORMALIZED TO p-p
p SIDE
0
5
10
15
20
25
30
35
40
-2
-1
0
1
2

Fig. 7

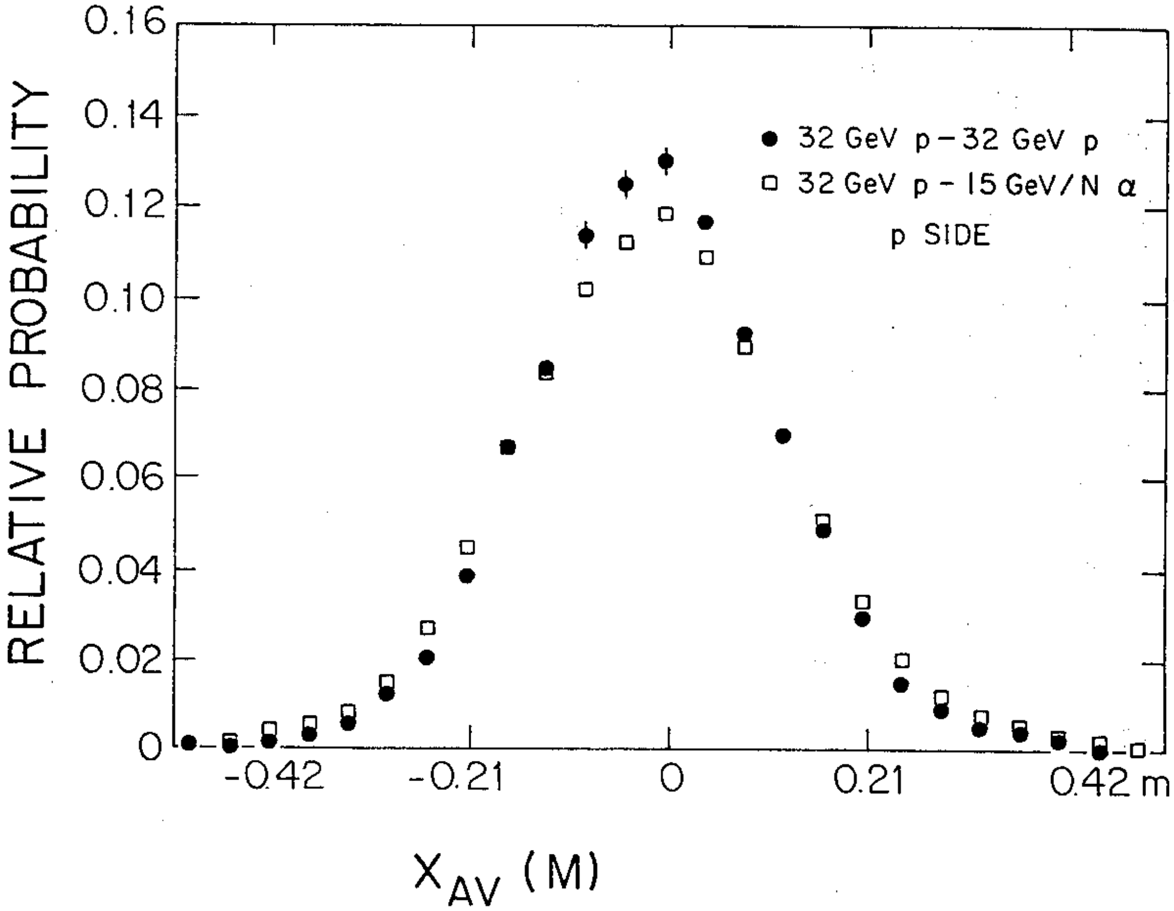

RELATIVE PROBABILITY
0.16
0.14
0.12
0.10
0.08
0.06
0.04
0.02
0
● 32 GeV p – 32 GeV p
□ 32 GeV p – 15 GeV/N α
p SIDE
-0.42
-0.21
0
0.21
0.42 m
X_AV (M)

Fig. 8

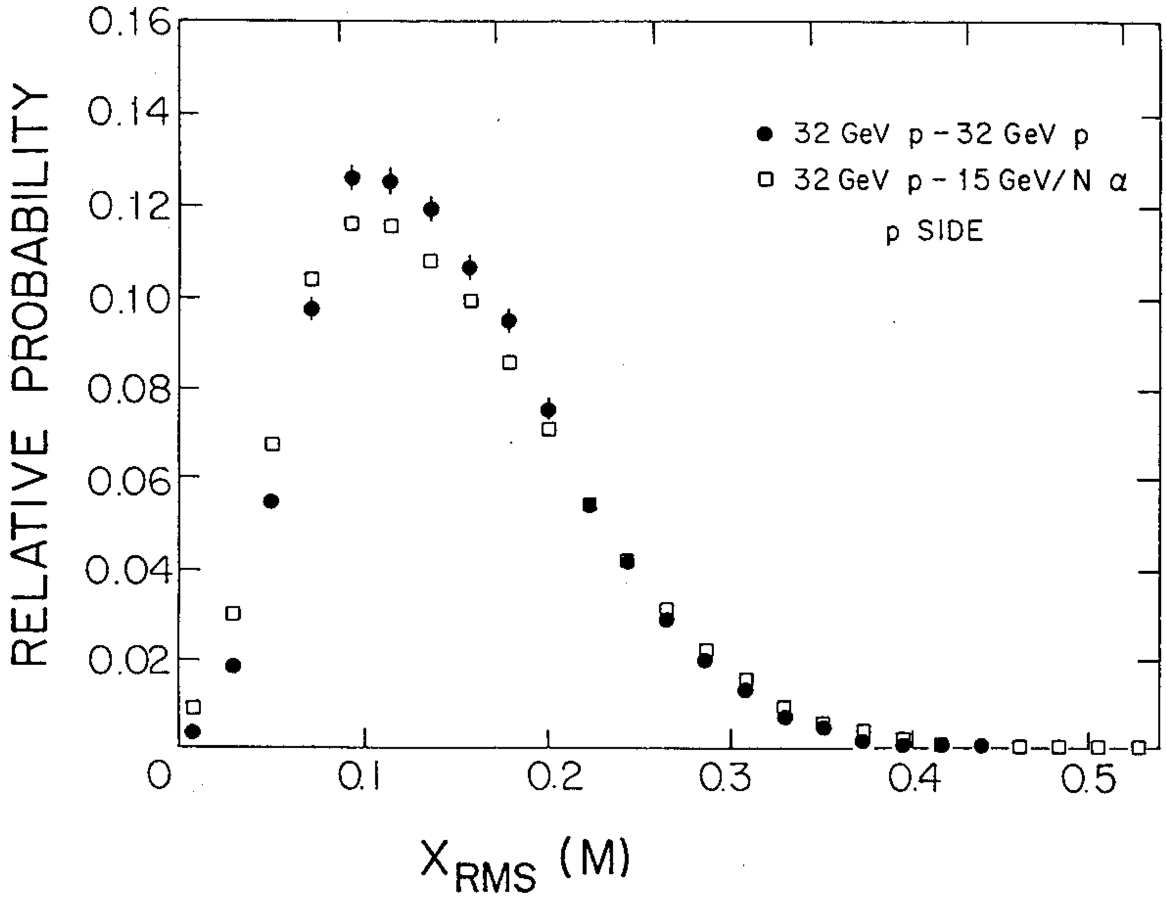
RELATIVE PROBABILITY
0.16
0.14
0.12
0.10
0.08
0.06
0.04
0.02
0
0.1
0.2
0.3
0.4
0.5
32 GeV p - 32 GeV p
32 GeV p - 15 GeV/N α
p SIDE
X RMS (M)

Fig. 9

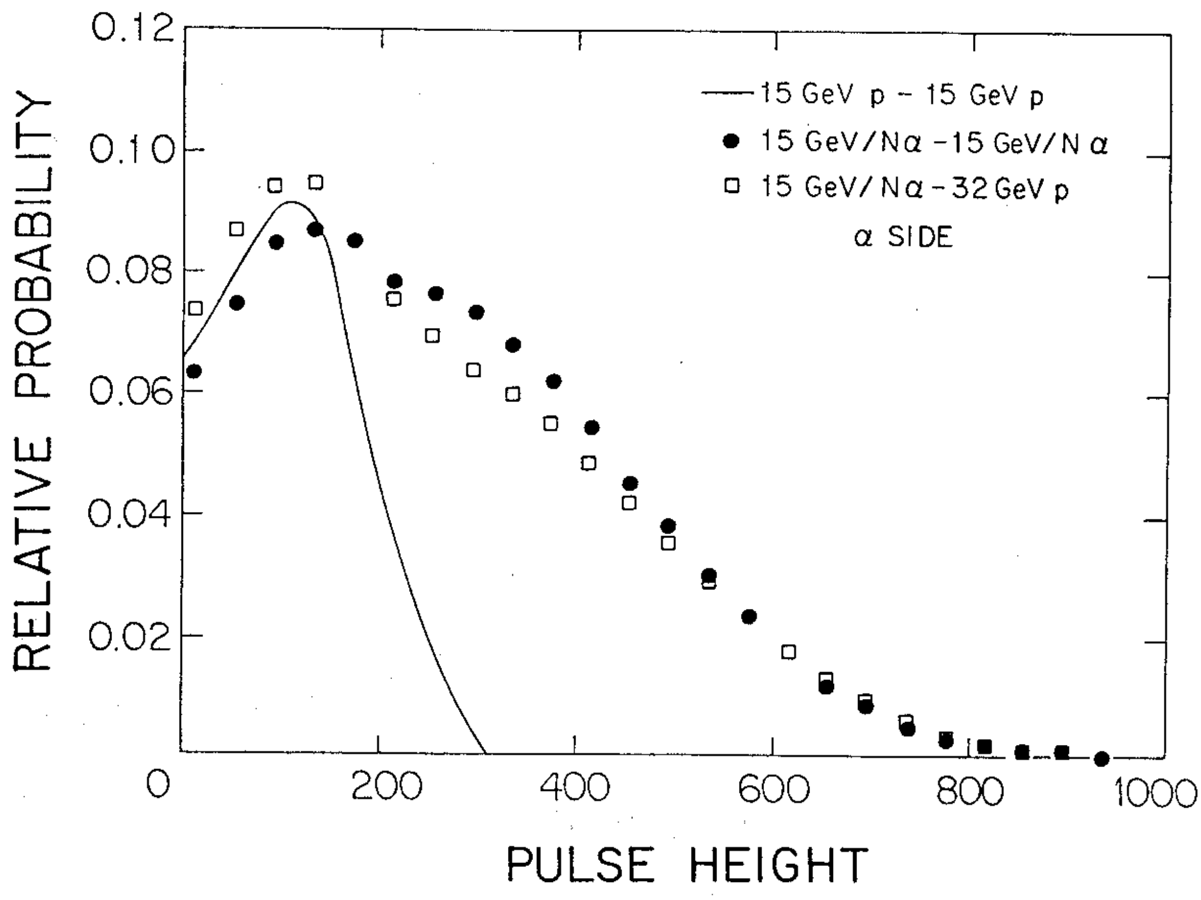

0.12
0.10
0.08
0.06
0.04
0.02
RELATIVE PROBABILITY
0
200
400
600
800
1000
PULSE HEIGHT
15 GeV p - 15 GeV p
15 GeV/Nα -15 GeV/N α
15 GeV/Nα -32 GeV p
α SIDE

Fig. 10

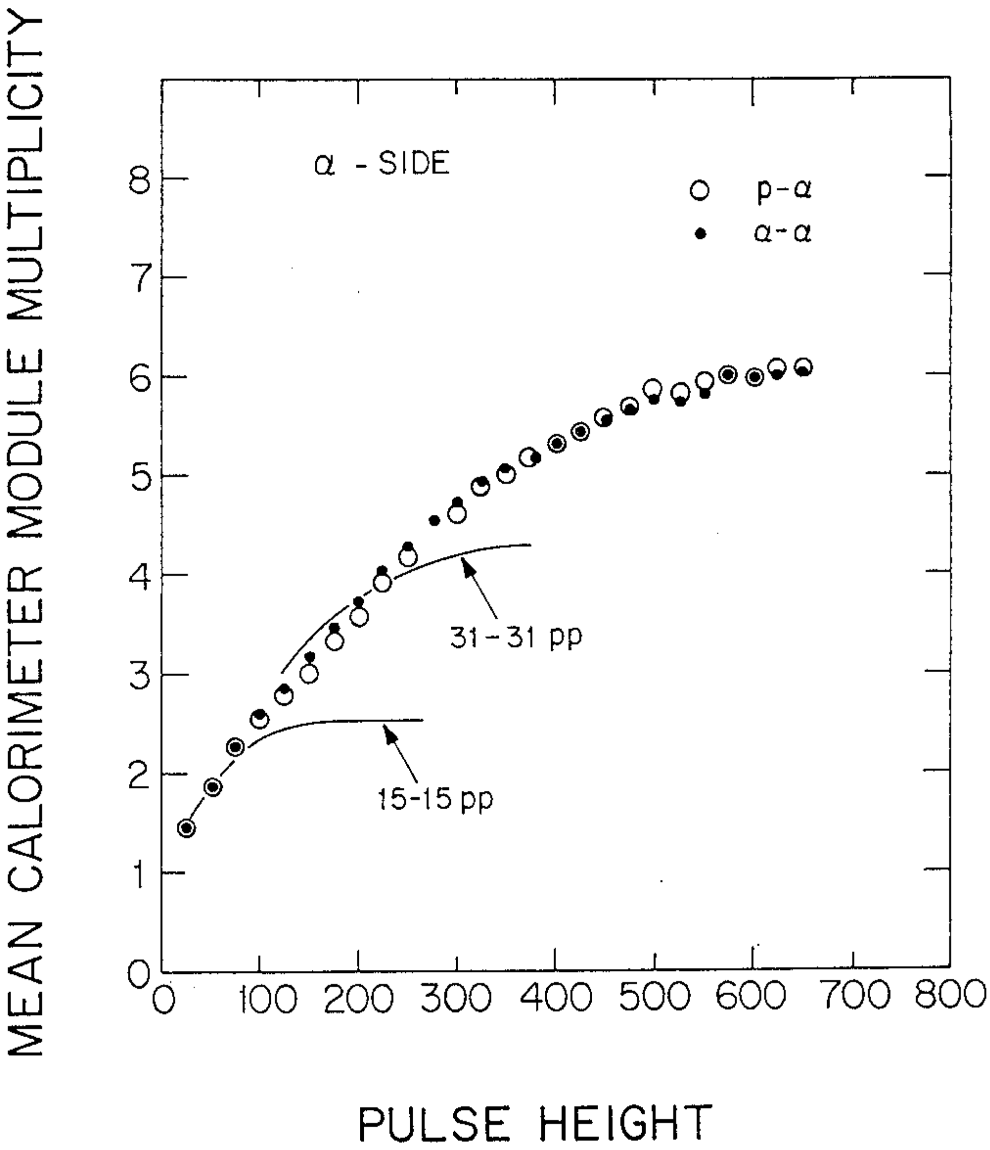
MEAN CALORIMETER MODULE MULTIPLICITY
α - SIDE
p-α
α-α
31-31 pp
15-15 pp
0
1
2
3
4
5
6
7
8
0
100
200
300
400
500
600
700
800
PULSE HEIGHT

Fig. 11

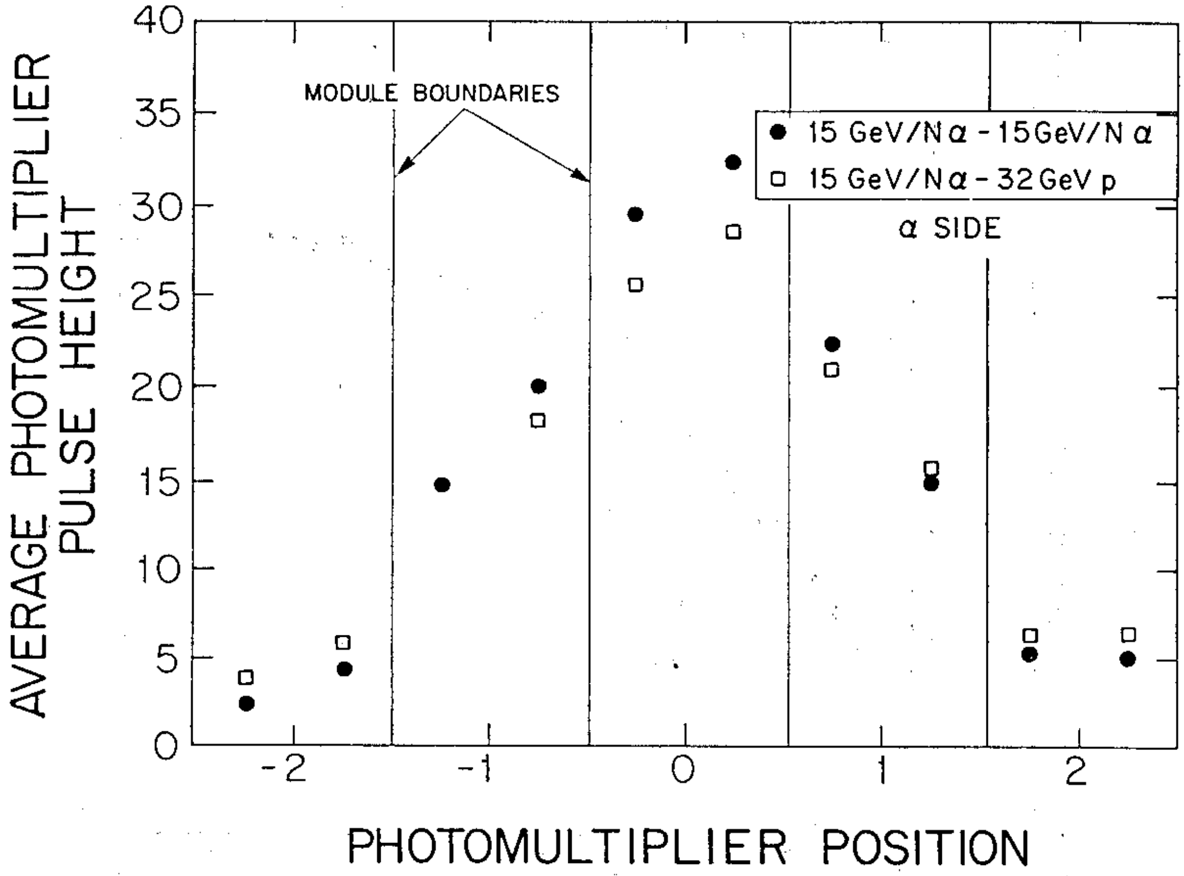

40
35
30
25
20
15
10
5
0
-2
-1
0
1
2
MODULE BOUNDARIES
15 GeV/N α - 15 GeV/N α
15 GeV/N α - 32 GeV p
α SIDE
AVERAGE PHOTOMULTIPLIER PULSE HEIGHT
PHOTOMULTIPLIER POSITION

Fig. 12

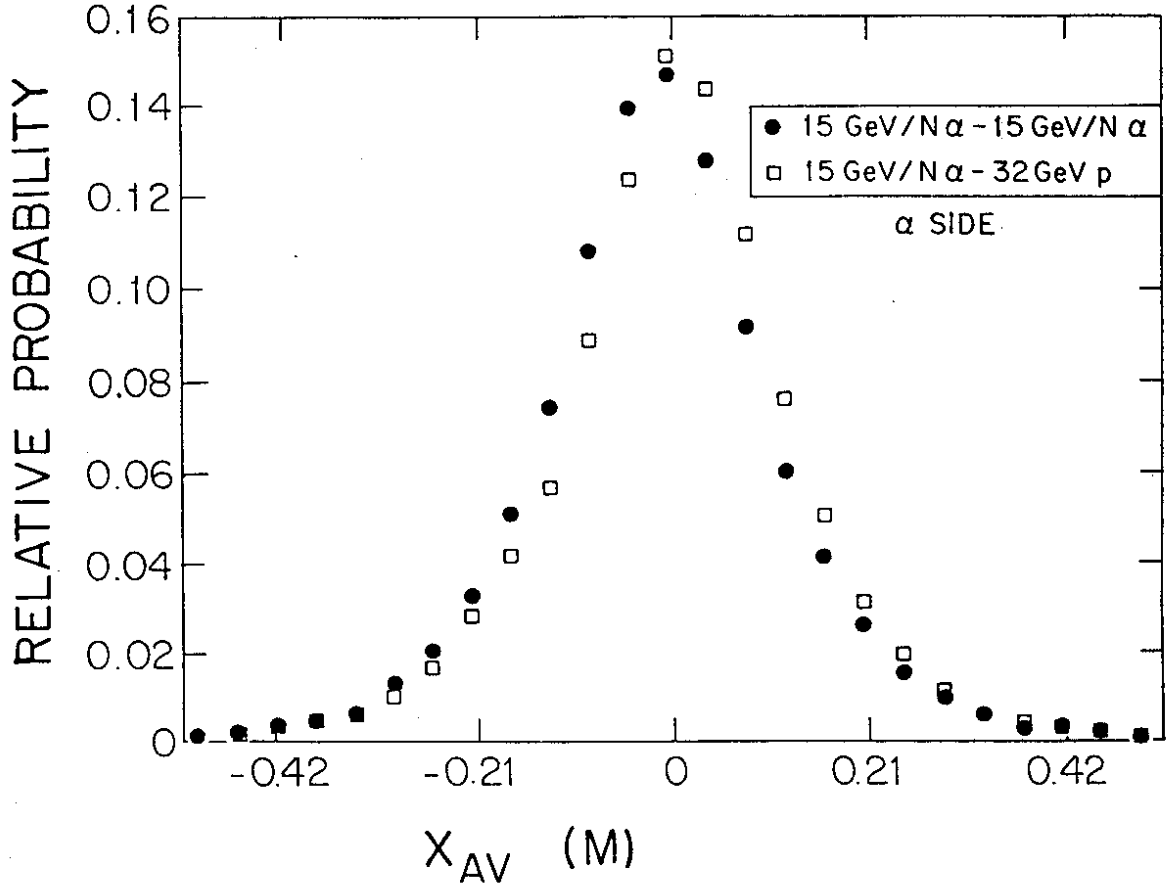
RELATIVE PROBABILITY
0.16
0.14
0.12
0.10
0.08
0.06
0.04
0.02
0
● 15 GeV/N α - 15 GeV/N α
□ 15 GeV/N α - 32 GeV p
α SIDE
-0.42
-0.21
0
0.21
0.42
X_AV (M)

Fig. 13

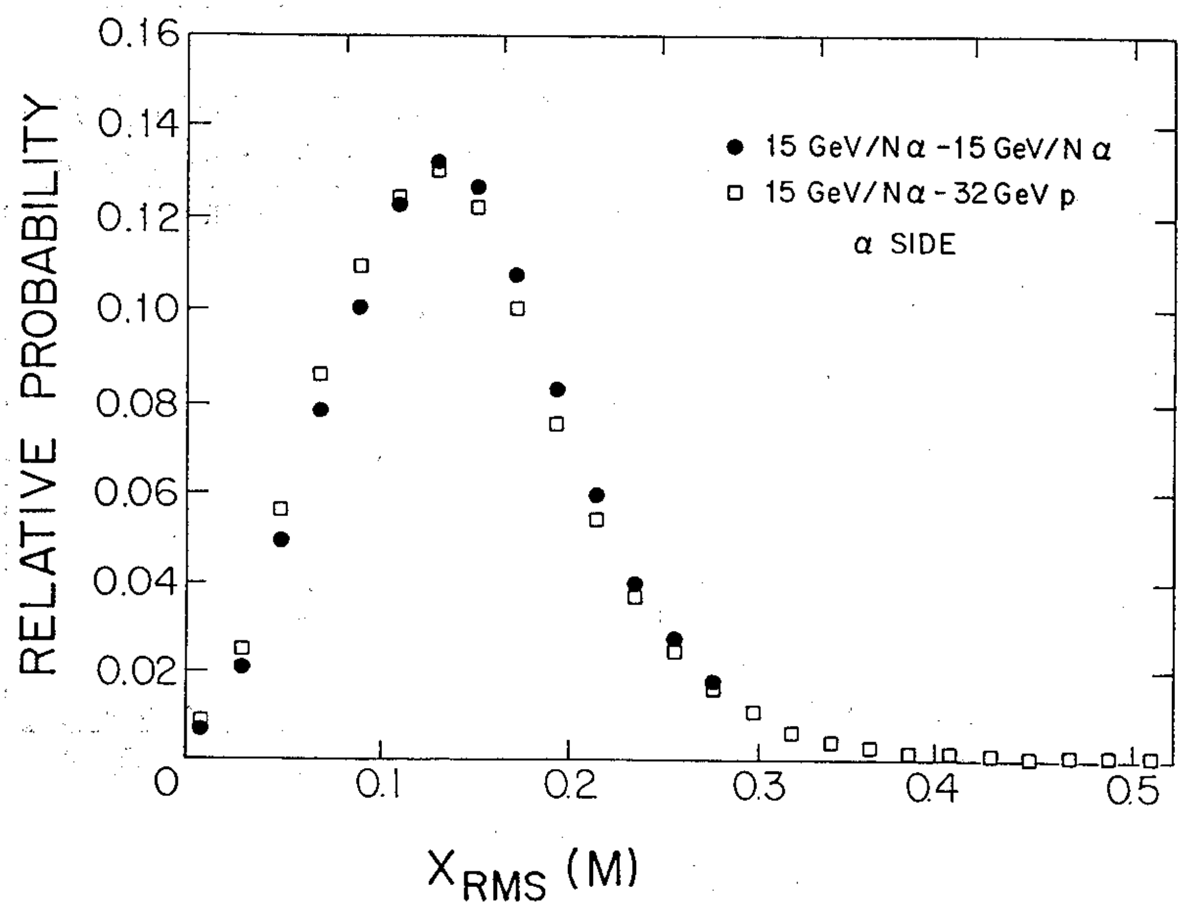

RELATIVE PROBABILITY
0.16
0.14
0.12
0.10
0.08
0.06
0.04
0.02
0
0.1
0.2
0.3
0.4
0.5
15 GeV/N α -15 GeV/N α
15 GeV/N α - 32 GeV p
α SIDE
X_{RMS} (M)

Fig. 14